

Thermally assisted flux flow in MgB₂: strong magnetic field dependence of the activation energy

A. SIDORENKO*†¶#, V. ZDRAVKOV†‡, V. RYAZANOV‡,
S. HORN§, S. KLIMM§, R. TIDECKS§, A. WIXFORTH§,
TH. KOCH¶ and TH. SCHIMMEL¶#

†Institute of Applied Physics, MD-2028 Kishinev, Moldova

‡Institute of Solid State Physics, RU-142432 Chernogolovka, Russia

§Institut für Physik, Universität Augsburg, D-86159 Augsburg, Germany

¶Institute of Nanotechnology (INT), Forschungszentrum Karlsruhe,
D-76021 Karlsruhe, Germany

#Institute of Applied Physics, Universität Karlsruhe,
D-76128 Karlsruhe, Germany

The origin of the resistive transition broadening of superconducting MgB₂ thin films is investigated. Thermally activated flux flow is found to be responsible for the resistivity in the vicinity of the critical temperature. The activation energy for flux motion is observed to have an extraordinary strong dependence on the magnetic field. The results are discussed.

1. Introduction

The discovery of superconductivity in MgB₂, a material which has a hexagonal layered crystal structure and has the highest critical temperature, $T_c = 39$ K, found for an intermetallic superconducting compound [1], has raised questions about its transport properties. This strong type-II superconductor with a large Ginzburg–Landau parameter, $\kappa \approx 26$, a magnetic penetration length, $\lambda(0) = 140\text{--}180$ nm [2] and short coherence lengths, $\xi_c(0) = 2.3$ nm, $\xi_{ab}(0) = 6.8$ nm [3] has a rather high critical current density up to $j_c \sim 1.6 \times 10^7$ A cm⁻² at 15 K [4]. The latter finding makes this novel superconductor very attractive for technical applications. On the other hand, a broadening of the superconducting transition, as found in resistivity measurements, would severely limit potential applications for MgB₂. Therefore, it is important to study the mechanisms that cause the broadening.

Broadening of superconducting transitions in the presence of magnetic fields can be due to several different reasons. Broadening may be caused by inhomogeneous microstructures in the polycrystalline samples, which have additional phases with

*Corresponding author. Email: anatoli.sidorenko@int.fzk.de

different T_c . Moreover, fluctuations play an important role in the vicinity of the superconducting transition, especially for low-dimensional and layered superconductors with short coherence lengths and high T_c 's, such as MgB_2 . Finally, thermally activated dissipation due to vortex lines motion may also broaden the transition.

Improving the sample preparation can eliminate broadening of the superconducting transition by inhomogeneities. Fluctuations and vortex-line motions are of fundamental nature and, therefore, have been the subjects of both experimental and theoretical investigations. The broadening of the superconducting transition by fluctuations was investigated in homogeneous high-quality MgB_2 films [5] and single crystals [6].

There exists a lack of information concerning the broadening of the resistive transition due to thermally activated flux creep or flux flow (TAFF) processes below the critical temperature for MgB_2 . In a type-II superconductor in the mixed state, the flux lines are fixed at "pinning centres", e.g. at defects or impurities. The main mechanism for flux creep, which broadens the resistive transition in magnetic fields, is thermal activated motion of flux-lines over the energy barrier, U_0 , of the pinning centre [7].

The layered structure of MgB_2 is expected to influence the magnetic flux penetration and motion leading to a broadening of the resistive transition similar to the case of high- T_c superconductors [7, 8] and artificially multilayered systems [9, 10]. On the other hand, magnesium diboride exhibits an anomalous magnetic behaviour with dendritic magnetic instabilities for vortex penetration [11] and "noise-like" jumps of the magnetization in an applied magnetic field [12], which should influence the resistive behaviour of this novel superconducting material.

The present work reports an experimental investigation of the broadening of the resistive transition of magnesium diboride thin films, caused by the TAFF mechanism.

2. Experiment

2.1. Sample preparation

MgB_2 films with a thickness of 100–10 000 nm were fabricated by DC-magnetron sputtering from Mg– MgB_2 composite targets (target diameter 32 mm, thickness 5 mm) prepared by a hot-pressing procedure from 99.9% purity Mg powder and 98% purity MgB_2 powder (Alfa Aesar). The films were deposited on (100)-oriented sapphire substrates, and on (128° rot)- LiNbO_3 substrates. During the sputtering process, the substrate temperature was kept at approximately 150°C. The deposition rate was 1.3 nm s⁻¹. Next, the deposited film was annealed *ex situ* at 850°C in a Mg vapour atmosphere. An X-ray diffraction study revealed a textured (101)-oriented structure of the films deposited on sapphire substrates, and polycrystalline films deposited on LiNbO_3 . Using a diamond cutter, samples were cut from the deposited films in the form of 1.5 mm wide strips. Platinum wires with 50 μm diameter were attached with silver paste for four-probe resistance measurements.

2.2. SEM and AFM characterization of the samples

A Gemini-982 system from Leo was used for scanning electron microscopy (SEM). The analysis of the SEM images was made with Leo software. Atomic force

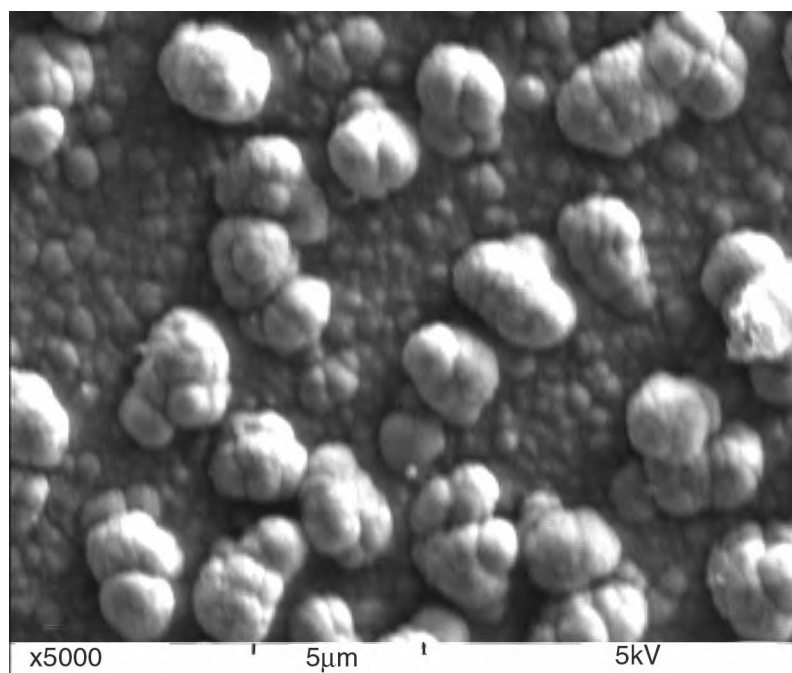


Figure 1. Electron microscope (SEM) image of 2.5 μm thick MgB_2 film on a LiNbO_3 substrate (scan size $20\ \mu\text{m} \times 15\ \mu\text{m}$, 5 kV); a rough island covered surface with a wide distribution of island size up to 5 μm were imaged.

microscopy (AFM) measurements were made using a Nanoscope-III/IIIa driven Multimode Systems equipped with $130\ \mu\text{m}$ vertical engage scanners and with both commercial and home built phase imaging units. The contact mode experiments were performed with type A “CSC21” silicon cantilevers from NT/MDT (resonance frequency 15 kHz, force constant $0.12\ \text{Nm}^{-1}$) at a typical force load of approx. 5 nN. For intermittent contact mode, type A “NSC15” silicon cantilevers (resonance frequency 325 kHz, force constant $40\ \text{Nm}^{-1}$) from the same company were used at a set point of 0.75. All AFM measurements were made under ambient conditions. The statistical analysis of the AFM images was made with SPIP software from Image-Met.

The SEM study shows a rather rough morphology of the films deposited on LiNbO_3 substrates. These films have a trigonal crystal structure, which does not match with the hexagonal structure of MgB_2 . Figure 1 presents an SEM image of an MgB_2 film deposited on LiNbO_3 . It shows that the grain size varies over a wide range, running between $0.2\ \mu\text{m}$ and $6\ \mu\text{m}$. AFM shows that the surface corrugation of the films deposited on the LiNbO_3 substrates exceed $5\ \mu\text{m}$.

The SEM investigations of MgB_2 films deposited on single crystalline (100) sapphire substrates (not shown here) exhibit a homogeneous microstructure with a very smooth surface, in contrast with the films deposited on LiNbO_3 . These smooth films were investigated by AFM to get detailed information about surface topography and roughness. In addition, phase imaging and lateral force microscopy were used to examine material contrast in order to prove the absence of other phases or foreign materials on the sample surfaces.

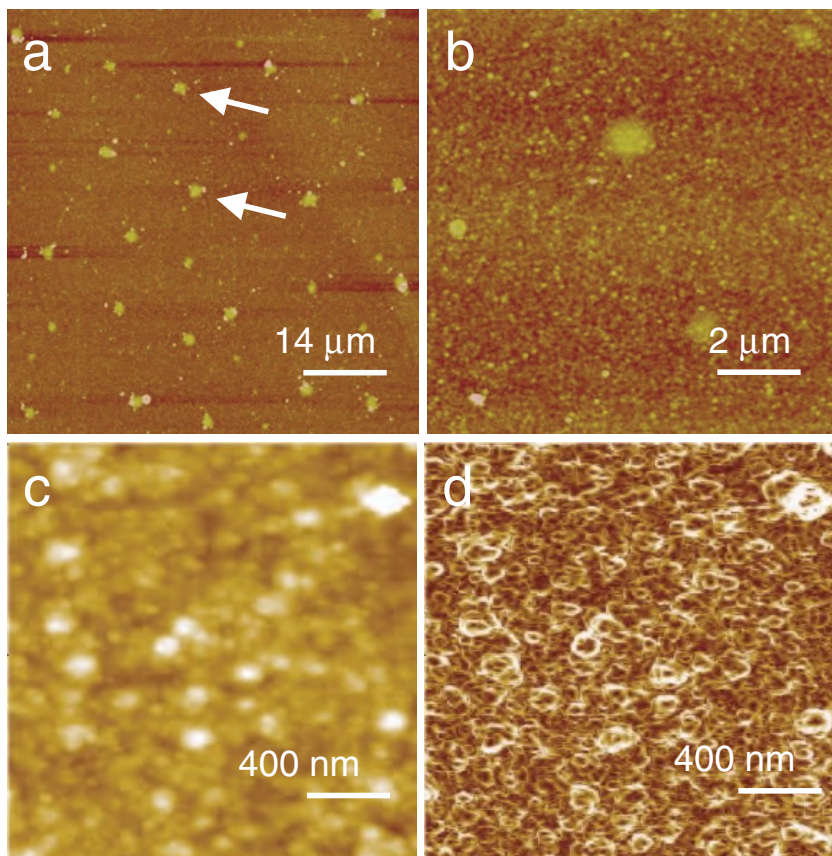


Figure 2. Atomic force microscopy images taken from the surface of a 400 nm thick MgB_2 film on (100) sapphire substrate: (a) tapping mode, scan size: $68 \mu\text{m} \times 68 \mu\text{m}$, z-scale 100 nm, RMS roughness $8.2 \pm 1.5 \text{ nm}$; (b) contact mode, scan size: $10 \mu\text{m} \times 10 \mu\text{m}$, z-scale 100 nm, RMS roughness $6.3 \pm 1.2 \text{ nm}$; (c) contact mode, scan size: $2 \mu\text{m} \times 2 \mu\text{m}$; z-scale 100 nm, RMS roughness $6.3 \pm 1.2 \text{ nm}$; (d) derivative of data of image 2c to highlight the island boundaries (z-scale = max. slope: 83°). The surface consists homogeneously of small islands with an average diameter of $49 \pm 15 \text{ nm}$ (c, d). In addition, uniformly distributed island groups (two of them marked with arrows) with a size up to $3 \mu\text{m}$ can be seen (a, b). These groups consist of densely packed islands with an average size of 50 nm. No significant material contrast was found in tapping mode phase imaging and contact mode friction force images.

The AFM images of the surface for a 400 nm thick MgB_2 film on sapphire substrate (figure 2) were taken at several different sample positions, both in the contact mode and tapping mode. The surface is homogeneously covered with flat islands (average height: 13 nm) with an average diameter of 50 nm (figure 2c and 2d). The results show this planar structure exists even for big scan sizes (figure 2a). Uniformly distributed island groups (figure 2a and 2b) with diameters between 100 nm and $3 \mu\text{m}$, a height of about 100 nm and a typical group to group distance of about $12 \mu\text{m}$ (figure 2a) are located on the surface of the film. These groups also consist of islands of an average size of 50 nm. The area coverage of the sample surface with these island groups is approximately 11%. Tapping mode phase imaging [13] and friction force microscopy [14] did not show any significant material

contrast on the film surface. The absence of differences in phase imaging shows that the values for adhesion and elasticity stay the same all over the observed surface areas. In addition, the results of the friction force microscopy show a constant material contrast in these areas, too. This accentuates the homogeneity of the investigated sample surfaces. The RMS values of the roughness of the MgB₂ films on sapphire substrate are between 6.3 nm and 8.2 nm. This fact, together with the absence of the material contrast, demonstrates the smooth and homogeneous character of the film.

2.3. Resistance measurements

Resistivity measurements, $\rho(T)$, of the MgB₂ samples were performed by a conventional four-probe method using an AC resistance bridge (Linear Research, LR700) in a ⁴He cryostat (Oxford Instruments) equipped with a 12 T superconducting solenoid. The temperature T was measured with a carbon-glass thermometer with an accuracy of 1–5 mK. The critical temperature T_c was determined from the mid-points of the $\rho(T)|_{B=\text{const}}$ curves.

3. Results and discussion

Figure 3 shows the resistive transitions $\rho(T)$ at several magnetic fields, B , oriented perpendicular to the MgB₂ film plane, for a sample on a sapphire substrate. The transition width is about 0.3 K in zero and low magnetic fields but increases up to ~2 K at high fields. Similar resistive transitions were measured for samples on LiNbO₃ substrates, showing slightly larger transition widths of about 0.9 K in zero magnetic field.

Usually, the broadening of the lower parts of the resistive transition, $\rho(T) < 0.01\rho_n$ (where ρ_n is the resistivity in the normal state just above the transition), in a magnetic field for layered superconductors is interpreted in terms of a dissipation of energy caused by the motion of vortices [8]. This interpretation is based on the fact that, for the low-resistance region, the resistance is caused by the creep of vortices so that the $\rho(T)$ dependences are thermally activated and are described by the equation

$$\rho(T, B) = \rho_0 \exp[-U_0/k_B T]. \quad (1)$$

Here, U_0 is the flux-flow activation energy, which can be obtained from the slope of the linear parts of an Arrhenius plot (according to equation (1)) and ρ_0 is a field-independent pre-exponential factor. Investigations of high- T_c superconductors and artificial multilayers showed that the activation energies exhibit different power-law dependences on the magnetic field, i.e. $U_0(B) \sim B^{-n}$ [7–9]. Since we used equation (1) with a temperature-independent U_0 to describe our experiments, the values of U_0 were deduced only from limited temperature intervals below T_c , where the Arrhenius plot (figure 4) of $\rho(T)$ consists of straight lines.

The linear behaviour of the resistance over five orders of magnitude indicates that the resistive behaviour of the MgB₂ film is caused by the TAFF-process as described by the Arrhenius law given in equation (1). The best fit of the experimental data $\rho(T)|_{B=\text{const}}$ to equation (1) yields values for the activation energy, which range from $U_0/k_B = 10\,000$ K in low magnetic fields down to 300 K in the high field region, as is shown in figure 5. Compared to the power law field dependence of the activation

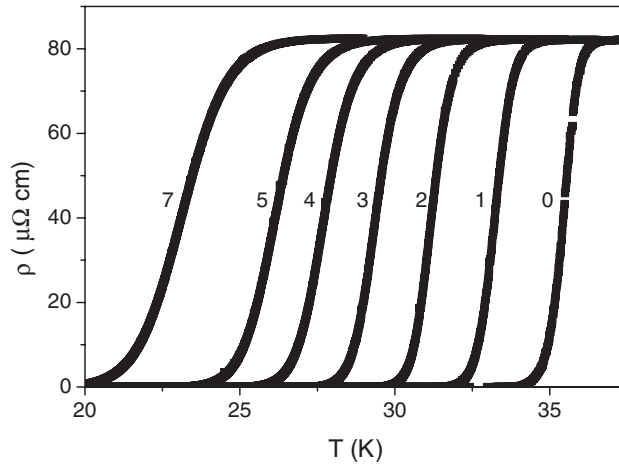


Figure 3. Resistive transitions $\rho(T)$ for a 400 nm thick MgB_2 film on sapphire substrate at different values of the magnetic field perpendicular to the film plane: curves 0 to 7 correspond to $B=0, 1, 2, 3, 4, 5,$ and 7 T , respectively.

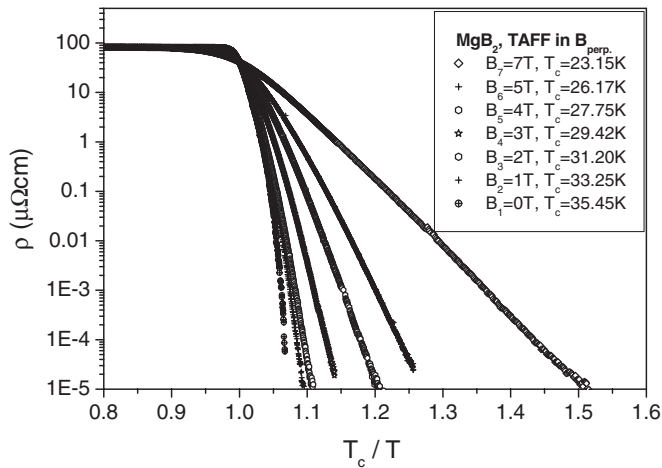


Figure 4. Arrhenius plot of $\rho(T)|_{B=\text{const}}$ for the sample presented in figure 3. From the slope of the linear parts of the curves the values of the activation energy U_0 are obtained. The Arrhenius plot presents the data of figure 3 as $\ln(\rho)$ against (T_c/T) .

energy $U_0(B) \sim B^{-n}$ with the exponent $n \leq 1$ that are usually observed for other layered systems [8–10, 15, 16], MgB_2 shows a much stronger field dependence in the high magnetic field region ($B > 1\text{ T}$). This is clearly demonstrated in figure 5, where our data for MgB_2 are shown together with a typical $U_0(B)$ dependence for a high- T_c superconductor (data for a Bi-Sr-Ca-Cu-O sample taken from Palstra *et al.* [15]).

The rapid decrease of the activation energy for MgB_2 for fields $B > 1\text{ T}$ reflects a dramatic loss of the current carrying capabilities of this superconductor with increasing magnetic field. This rapid decrease is due to the weakening of the flux-line pinning. A possible reason for the unusually strong magnetic field dependence of the activation energy of the TAFF process in MgB_2 may be due to the appearance of

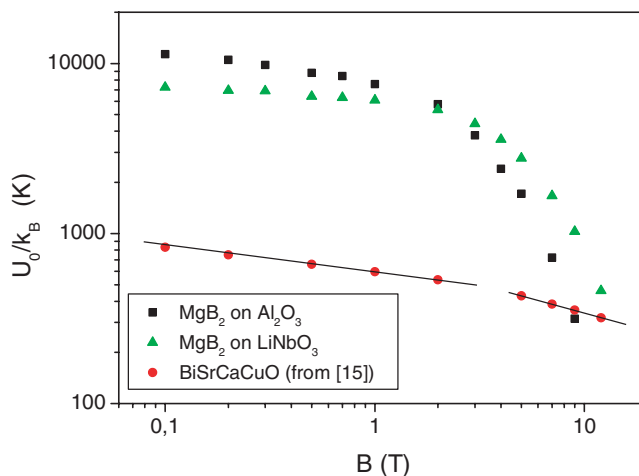


Figure 5. Dependence of the activation energy, U_0/k_B , on magnetic field for the investigated samples (solid squares, 400 nm thick MgB_2 film deposited on sapphire; solid triangles, 2.5 μm thick film deposited on LiNbO_3). For comparison, the weak power-law dependence $U_0 \sim B^{-n}$, $n = 1/6$ and $n = 1/3$ for two linear parts of the $U_0(B)$ dependence, for a high- T_c superconductor (solid circles, data for Bi-Sr-Ca-Cu-O sample taken from [15]) is given.

thermomagnetic instabilities of the type considered by Mints and Rakhmanov [17]. These instabilities would lead to a complex flux dynamics, such as the dendritic flux instability in MgB_2 films, found recently [11] for c-axis textured films in a magnetic field oriented perpendicular to the plane of the film. The magneto-optical measurements demonstrate a “fractal-like” structure of the flux penetration with an amount of the flux-dendrite density, which shows a strong increase with increasing magnetic field. Mesoscopic flux jumps appear as a result of the thermomagnetic instability [18]. More generally, as analysed by Tinkham [19], thermal instabilities may have disastrous consequences for superconducting magnets and cables because the materials may rapidly heat up due to the dissipation of energy associated with flux creep. Therefore, for thermal stability of a superconductor, an increase in local heat production due to more rapid flux motion has to be met by an increased outflow of heat to the surrounding material.

From the reported results, one may conclude that the strong magnetic field dependence of the activation energy $U_0(B)$ is an intrinsic property of MgB_2 , because a quite similar strong $U_0(B)$ dependence was observed both for samples with a homogeneous smooth microstructure prepared on sapphire substrate and for very rough films deposited on LiNbO_3 substrate.

The unusual flux creep behaviour of magnesium diboride needs further investigation, especially in view of future applications, for which an increase of the flux line pinning and a thermal stabilization of wires and tapes are necessary for electrical transport with high current density.

Acknowledgements

The authors are grateful to P. Ziemann, J. Eisenmenger, E.-H. Brandt and A. Zaikin for useful discussions, and to A. Rossolenko and O. Kroemer for

experimental assistance, as well as to the A. v. Humboldt Foundation for the donation of “Coolpower-4.2GM” and “PLN-106” refrigerators. This work was partially supported by BMBF, Project Nr.MDA02/002 and by the Deutsche Forschungsgemeinschaft within the DFG-Center for Functional Nanostructures CFN as well as by INTAS, Project Nr. 03-55-1856.

References

- [1] J. Namagatsu, N. Nagakawa, T. Muranaka, Y. Zenitani and J. Akimitsu, *Nature* **410** 63 (2001).
- [2] D.K. Finnemore, J.E. Ostenson, S.L. Bud'ko, G. Lapertot and P.C. Canfeld, *Phys. Rev. Lett.* **86** 2420 (2001).
- [3] Y. Eltsev, S. Lee, K. Nakao, N. Chikumoto, S. Tajima, N. Koshizuka and M. Murakami, *Phys. Rev.* **65** 140501 (2001).
- [4] H.-J. Kim, W.N. Kang, E.-M. Choi, M.-S. Kim, K.H.P. Kim and S.-I. Lee, *Phys. Rev. Lett.* **87** 087002 (2001).
- [5] A.S. Sidorenko, L.R. Tagirov, A.N. Rossolenko, N.S. Sidorov, V.I. Zdravkov, V.V. Ryazanov, M. Klemm, S. Horn and R. Tidecks, *JETP Letters* **76** 20 (2002).
- [6] T. Masui, S. Lee and S. Tajima, *Phys. C: Superconductivity* **383** 299 (2003).
- [7] Y. Yeshurn and A.P. Malozemoff, *Phys. Rev. Lett.* **60** 2202 (1988).
- [8] T.M. Palstra, B. Batlogg, R.B. van Dover, L.F. Schneemeyer and J.V. Waszchak, *Phys. Rev. B* **41** 6621 (1990).
- [9] N.Y. Fogel, V.G. Cherkasova, O.A. Koretzkaya and A.S. Sidorenko, *Phys. Rev. B* **55** 85 (1997).
- [10] J.M. Graybeal and M.R. Beasley, *Phys. Rev. Lett.* **56** 173 (1986).
- [11] T.H. Johansen, M. Bazilevich, D.V. Shantsev, P.E. Goa, Y.M. Galperin, W.N. Kang, H.J. Kim, E.M. Choi, M.-S. Kim and S.I. Lee, *Europhys. Lett.* **59** 599 (2002).
- [12] S. Jin, H. Mavoori, C. Bower and R.B. van Dover, *Nature* **411** 563 (2001).
- [13] G.K.H. Pang, K.Z. Baba-Kishi and A. Patel, *Ultramicroscopy* **81** 35 (2000).
- [14] A. Pfrang, K. J. Hüttinger and T. Schimmel, *Surf. Interface Analysis* **33** 96 (2002).
- [15] T.T.M. Palstra, B. Batlogg, L.F. Schneemeyer and J.V. Waszczak, *Phys. Rev. Lett.* **61** 1662 (1988).
- [16] O. Brunner, L. Antognazza, J.-M. Triskone, L. Mieville and O. Fischer, *Phys. Rev. Lett.* **67** 1354 (1991).
- [17] R.G. Mints and A.L. Rakhmanov, *Rev. Mod. Phys.* **53** 551(1981).
- [18] A.V. Bobyl, D.V. Shantsev, Y.M. Galperin, A.A.F. Olsen, T.H. Johansen, W.N. Kang and S.I. Lee, cond-mat/0304603.
- [19] M. Tinkham, *Introduction to Superconductivity*, 2nd edn (McGraw Hill, New York, 1996).